Internal laser-induced dipole force at work in C_{60} molecule

Bhardwaj, V. R.; Corkum, P. B.; Rayner, D. M.

Publisher's version / Version de l'éditeur:
https://doi.org/10.1103/PhysRevLett.91.203004
Physical Review Letters, 91, 20, pp. 203004-1-203004-4, 2003-11-13

Internal Laser-Induced Dipole Force at Work in C_{60} Molecule

V. R. Bhardwaj, P. B. Corkum, and D. M. Rayner

Steacie Institute for Molecular Science, National Research Council, 100 Sussex Drive, Ottawa, Ontario, Canada K1A 0R6

(Received 9 June 2003; published 13 November 2003)

We show how the many electron response of a complex molecule to an intense laser field can be incorporated with the single active electron picture. This enables us to introduce an "over-the-barrier" model for C_{60}^{z+} ionization, valid for long wavelength light. Using infrared radiation, we confirm the model and also produce stable, highly charged C_{60} reaching C_{60}^{12+}, the highest charge state ever observed. At high intensities and high charge states the internal laser-induced dipole force and rapid charging lead to stress on the molecule. The interplay between the forces provides control and suggest strategies for reaching even higher charge states.

DOI: 10.1103/PhysRevLett.91.203004 PACS numbers: 33.80.Rv, 33.80.Wz, 36.40.Qv, 78.67.Bf

Optimized by genetic algorithms, intense femtosecond laser pulses with complex temporal shapes are known to control unimolecular chemical processes, sometimes of considerable complexity [1–3]. The physical mechanisms responsible for control remain obscure in many cases. Progress has been impeded by the inherently multielectron nature of large molecules and the simultaneous presence of both ionization and dissociation in experiments. Using long wavelength light, we predict and measure how the multielectron response in C_{60} couples to the ionizing electron and to the molecular framework. In so doing, we show how a distributed internal laser-induced dipole force (related to bond softening in small molecules [4]) arises in large molecules. Laser-induced dipole forces are traditionally used to trap atoms [5,6], control the external variables of molecules [7,8], or manipulate biological particles via optical tweezers [9,10]. The internal force provides a means of controlling the internal degrees of freedom of molecules that is unique to short intense laser pulses.

We work on C_{60} because it is a large molecule with high symmetry and simple electronic structure. It allows us to add complexity to our experiments in steps. First we remove one electron at a time. Using a metal sphere model of C_{60}^{z+} that treats a single active electron and includes the laser-induced dipole moment and the image charge, we calculate the "over-the-barrier" intensity needed for ionization of C_{60}^{z+} ($z = 1 - 9$). For $z = 3 - 9$, the model agrees with the saturation intensities that we measure. In this way we clarify the long-standing problem of why molecules (and other complex materials) ionize at higher fields than atoms of the same ionization potential [11–13]. As we increase the peak intensity to 10^{15} W cm^{-2}, we observe stable C_{60}^{12+} in our mass spectrometer, the highest charge state of C_{60} ever observed. The stress applied to the molecular framework by the charge leads to a vibrational wave packet. A single control pulse timed to produce a dipole force in the opposite direction to the wave packet motion offers a means of extracting coherent vibrational energy from the molecule. It may allow even higher charge states to be reached.

We use light in the 1.2–2.2 μm range. This further simplifies the problem by placing us in a regime where ionization is quasistatic [14]. We carry out the experiment in a Wiley-McLaren time-of-flight mass spectrometer (TOFMS). Differential pumping allows the source chamber to be operated at up to 10^{-5} Torr, while maintaining the flight chamber under high vacuum. A 500 mm slit at the entrance to the drift region of the TOFMS collects the ions produced in the focal volume. We evaporate C_{60} powder (purity 99.5%, MER Corporation) in an oven at a temperature of 550 °C to produce an effusive beam of C_{60}. The neutral C_{60} beam is partly collimated by passing through a 1 mm diameter pinhole located 2 cm above the oven. The oven is located below the ion optics of the spectrometer midway between the electrodes. A liquid nitrogen trap above the spectrometer ensures that C_{60} molecules are not adhered onto the parabolic mirror and vacuum chamber walls.

We use a Ti:sapphire regenerative amplifier system of standard design (50 fs, 750 mJ, 800 nm, 500 Hz) to pump an optical parametric amplifier (OPA). We use a broad bandwidth cube polarizer to select the signal or idler from the OPA. The signal or idler energy is typically 75 mJ. We measure the pulse duration to be 70 fs at 1500 nm using a second harmonic frequency resolved optical gating and we use a Berek variable wave plate in $\lambda/4$ configuration to change the ellipticity of the laser polarization. For intensities up to $\sim 3 \times 10^{14}$ W cm^{-2} we focus with an $f/25$ lens. Under these conditions (beam waist of 17 μm FWHM and confocal parameter 605 μm) the 0.5 mm slit at the entrance to the drift region of the TOFMS collects only ions produced in the focal volume to simplify interpretation of intensity dependencies. By using an $f/2$ convex mirror, placed inside the chamber, we can increase the available intensity to 10^{15} W cm^{-2}.

We find ionization of C_{60} at long wavelengths is almost fragment free and highly charged cations are generated. In contrast, at 800 nm the maximum charge state reached using pulses down to 35 fs is C_{60}^{3+} [15], while at 25 fs C_{60}^{5+} is observed [16]. Figure 1 shows the mass spectrum obtained at 10^{15} W cm^{-2}. The evidence for C_{60}^{10+} and C_{60}^{11+}

production is overwhelming [Fig. 1(b)]. We do not resolve the structure on the C_{60}^{12+} peak but the overall shape lets us make the assignment [Fig. 1(a)]. C_{60}^{12+} is at least stable over the 0.5 μs it spends in the acceleration region of the mass spectrometer. C_{60}^{12+} is two charge states higher than has been achieved before [17].

Our first challenge is to understand the multielectron response of C_{60}^{z+}. It determines the ionization dynamics and it is through the electronic response that the internal dipole force is exerted. We measure the intensity at which the ionization probability reaches saturation, $I_{\rm sat}$, for each charge state of C_{60}^{z+} [13,18]. The results are shown in Fig. 2.

To model C_{60}^{z+} ionization we work within the barrier suppression (BSI) or classical ionization approximation. Barrier suppression predicts saturation intensities in femtosecond ionization of rare-gas atoms [19]. The saturation intensity is identified with the minimum laser field required to suppress the Coulomb barrier below the ionization potential, IP. For an atom $I_{\rm sat} = (IP)^4/16z^2$ (atomic units). We treat C_{60} as a conducting sphere (CS) of effective radius $a = (a' + \delta a)$ where a' is the C_{60} radius and δa is the spillout [20,21]. We replace the Coulomb potential used for atomic ionization with the potential $\Phi(r)$ given by

$$\Phi(r) = -Er + \frac{a^3}{r^2}E - \frac{q}{4\pi\varepsilon}\left(\frac{a}{2(r^2 - a^2)} + \frac{z - \frac{a}{2r}}{r}\right), \quad (1)$$

where r is the distance from the center of the sphere [22]. As written, z is the final charge on C_{60}^{z+}. Physically the two terms in the bracket describe the potential of the electron due to its image charge and to z. The a^3E/r^2 term is due to the dipole induced in the sphere by the field. Note that a^3 is directly related to the polarizability, α, of the sphere. Thus the potential in Eq. (1) includes the finite size and the polarizability, two of the major differences between molecules and atoms. The solid curve and square data points in Fig. 2 compare the BSI saturation intensities found using the CS potential with the experimental $I_{\rm sat}$. For the BSI calculations we use IPs obtained by treating C_{60} as a molecular capacitor [20]. This approach has been validated by experiment for $z \leq 5$ [21]. The agreement between the experimental $I_{\rm sat}$ and the CS model is remarkable, especially for high charge states. The dashed curve in Fig. 2 shows $I_{\rm sat}$ obtained by omitting the induced-dipole term from $\Phi(r)$. The inset in Fig. 2 shows that the induced dipole raises the barrier by almost 10 eV at 10^{14} W cm^{-2}. It is a long-standing problem that large molecules (and other complex materials) are more difficult to ionize than one might expect from experience with atomic ionization and as predicted by single active electron models [11,13]. Our results show that, at least for C_{60}, this is a multielectron effect. Other atomic physics concepts appear to remain valid.

We now turn to the effect of the laser pulse on the nuclear degrees of freedom. Although there is little fragmentation visible in Fig. 1, there is some. We summarize the relevant observations. First, the fragmentation is isotropic with respect to the laser polarization axis. Second, highly charged parent molecules are more probable with circularly polarized light than with linear.

To gain insight into the fragmentation and survival of highly charged C_{60}^{z+} we use the metal sphere model for the electron response and a classical molecular mechanics model for the nuclear response. The charge distribution associated with the laser-induced dipole [22] leads to a

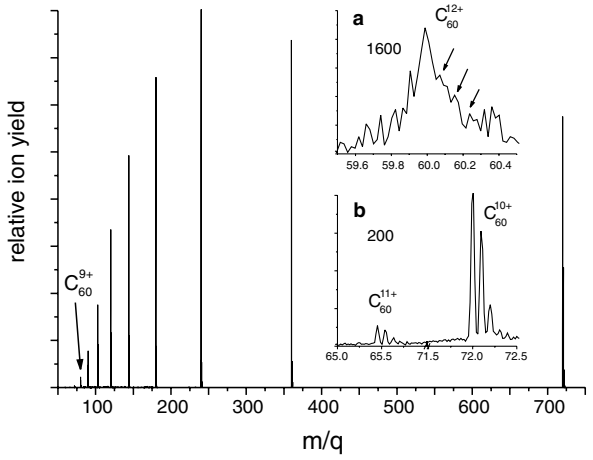

FIG. 1. Production of highly charged C_{60}^{z+} cations, $z \leq 12$, by intense (10^{15} W cm^{-2}), short (70 fs) infrared (1800 nm) laser pulses. The insets show the low m/q regions corresponding to C_{60}^{z+}, $z = 10$ to 12, at increased magnification. Highly charged C_{60} ions are distinguished from possible interfering lower charged ions, e.g., C_6^+ vs C_{60}^{10+} by their isotopomer distribution. The isotopomer ratio for C_{60}, $^{12}C_{60}$:$^{12}C_{59}{}^{13}$C:$^{12}C_{58}{}^{13}C_2$, is 1:0.65:0.21. Peak heights for $z < 9$ do not reflect mass abundances due to saturation.

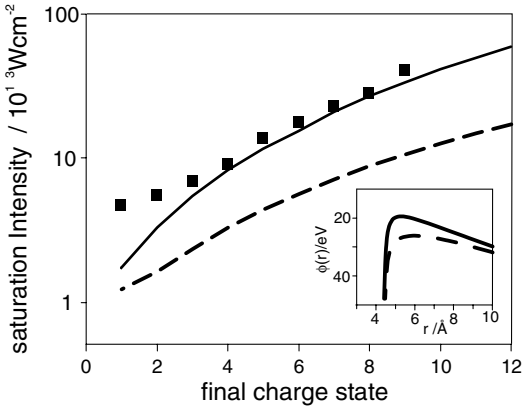

FIG. 2. Saturation intensities, $I_{\rm sat}$, for C_{60}^{z+} sequential multiionization by an intense laser, short laser pulse. The squares are the experimental values of $I_{\rm sat}$. The solid line shows $I_{\rm sat}$ predicted by the conducting sphere model. The dashed line shows the result of neglecting the dipole contribution. The inset shows the effect of the induced dipole on the ionization barrier.

distributed internal laser-induced dipole force. It pulls on the molecular framework as shown in Fig. 3 for linearly polarized light. We calculate the charge on each C atom, as a function of the instantaneous field, from the charge density at the atom's equivalent position on a conducting sphere. Assuming the atom occupies 1/60 of the surface of C_{60}, the charge, q_i, is given by $4\pi r^2\rho_i/60$, where $\rho_i = 3\varepsilon E\cos\theta$. The force on the ith atom due to the laser field, $\mathbf{F}_i$, is then given by $\mathbf{F}_i = q_i E_0[\mathbf{i}\cos(\omega t) + \epsilon\mathbf{j}\sin(\omega t)] \times \exp -t^2/\tau^2$ where τ is the half-width of the laser pulse at $1/e$, ω is the laser frequency, and ϵ is the ellipticity. We treat C_{60}^{z+} as a classical spring-mass network in a similar manner as has been used to analyze the rotation-vibration spectrum of neutral C_{60} [23]. We use their simplification that associates a single force constant, h, with the stretching of both the single and the double bonds and a single force constant, η, that describe C-C-C and C-C=C bending. Values for h (760 N/m) and η (70 N/m) are taken from the spring constants of benzene [23]. We follow the response of the spring-mass network to a short pulse by numerical integration in time using finite differences by the velocity Verlet method. The total force on each atom is the vector sum of $\mathbf{F}_i$ and the forces due to the distortion of the spring network calculated from Hooke's Law. The atoms start at rest at their equilibrium positions in C_{60}.

Solving the molecular dynamics model shows that a linearly polarized pulse sets up an oscillation between prolate and oblate forms of C_{60}. We identify this distortion as the lowest H_g normal mode of C_{60} both because this mode corresponds to the prolate/oblate motion and because the predicted period of oscillation (125 fs) is well matched to that known for the $H_g(1)$ mode of C_{60} at 273 cm^{-1} [24]. The H_g mode is accessible to our 70 fs pulse because its period is long enough for it to respond nonadiabatically. The work done, U, on the molecule by the induced-dipole force increases with laser intensity, as shown in Fig. 3. At 10^{15} W cm^{-2} U is 7 eV.

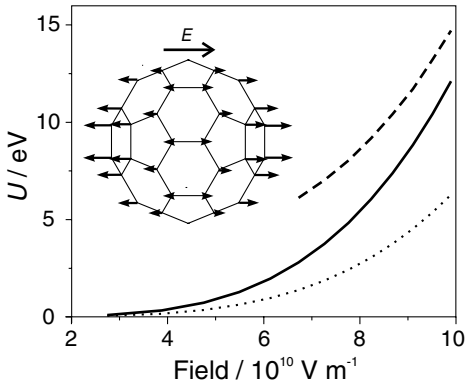

FIG. 3. Internal laser-induced dipole forces and the work they do, U, on the atoms of C_{60} in an electric field. The arrow lengths show how the forces increase toward the poles. U is shown as a function of intensity for linearly polarized (straight line) and circularly polarized (dotted line) laser pulses. Also shown, at relevant intensities, is the result of including the contribution of rapid Coulomb expansion for the case of C_{60}^{12+} (dashed line).

In circularly polarized light the induced-dipole force still acts but it does not lead to the absorption of as much energy from the laser field even though its intensity doubles (Fig. 3). The H_g mode is still the predominant mode excited but it is out of phase compared to the linear polarization case.

A second vibrational excitation mechanism also operates for high charge states. The high nonlinearity of multiphoton ionization means that charging is sudden. This exerts an impulsive force that acts to expand the molecule. As a result of sudden charging the molecule oscillates about a new equilibrium position where the Coulomb force expanding the shell is balanced by the increase in the stretching potential in the bonds. Delocalized over C_{60}, this is equivalent to exciting the symmetric $A_g(1)$ breathing mode that has a period of 67 fs [24]. We model the response due to the sudden charging of C_{60} by spreading the excess charge over all nuclei (i.e., the charge on each carbon atom is $z/60$) and summing all pairwise interactions to calculate the force on each atom for inclusion in the finite differences integration. The new equilibrium positions can be found either numerically, by taking the positions at the crossing point where the kinetic energy is maximum, or more directly from the relationship $R^2(1 - R) = U_0/h\sum x_0^2$, where R is the ratio of the C_{60} radius in the new equilibrium position to the original radius, U_0 is the Coulomb energy of the C_{60}^{z+} in the original geometry of C_{60}, and $\sum x_0^2$ is the sum of the squares of all the original bond lengths of the molecule. The internal energy deposited in the ion, U_s, is given by $U_s = h(1 - R)^2\sum x_0^2/2$ as long as the charging is sudden compared with the natural frequency of the motion it drives. We predict that 3.5 eV is deposited into C_{60}^{12+} by this mechanism.

The combination of the laser-induced dipole force and the Coulomb expansion can lead to significant excitation. After the pulse is over, the energy localized predominantly in the H_g and/or A_g modes will relax to the rest of the vibrational modes. If there is sufficient internal energy unimolecular dissociation can follow. The major dissociation channel for C_{60}^{z+} ions ($z > 3$) is asymmetric fission to form $C_{58}^{(z-1)}$ and C^{2+}. The barrier to this reaction drops with increasing z due to Coulomb repulsion. The balance between this dropping barrier and the increasing energy deposited by the laser with z determines the highest observable charge state. In C_{60}^{12+} the barrier is still high enough for it to survive at least 0.5 μs with an internal energy of 15 eV [5 eV initial thermal energy +10 eV (4 eV) due to the laser interaction with linearly (circularly) polarized light]. Fragmentation is limited to high charge states as sufficient energy is deposited only at the high intensities where they are the dominant species. The delayed dissociation results in the isotropic fragment

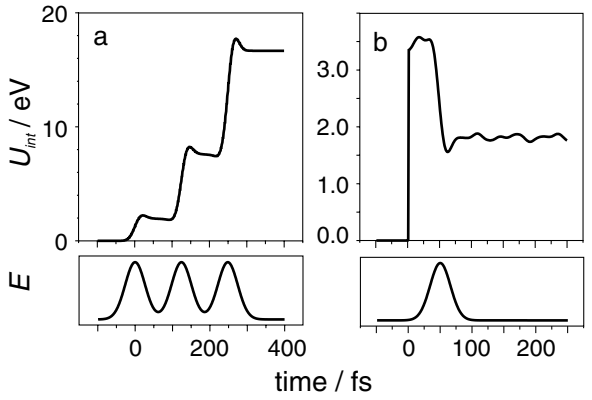

FIG. 4. Control of the internal energy, U_{int}, deposited in C_{60} during interaction with an intense laser field. (a) Energy deposited by a train of three 75 fs pulses through the induced dipole interaction. The pulse separation is timed to the period of the H_g mode of C_{60} (125 fs). (b) Removal of energy deposited in C_{60}^{12+} by Coulomb expansion using a 45 fs pulse timed to follow ionization by 49 fs, 3/4 the period of the A_g mode.

distribution that we observe. The greater stability of C_{60}^{z+} when produced with circularly polarized pulses is due to the reduced internal energy coupled to the molecule.

Combining wave packet motion with the internal laser induced-dipole force allows a new form of control that can be understood in classical terms as the work done on the molecule $U = \sum \mathbf{F}_i d\mathbf{s}_i$, where the sum is over all atoms in the molecule and $\mathbf{s}_i$ is the path length of the ith atom. Energy is transferred to (or from) the molecule if the force works parallel (or antiparallel) to the motion. We illustrate control by two examples for C_{60}. In the first, a train of three pulses, separated by the period of the H_g mode, couples 1.9, 5.6, and 9.5 eV for a total of 17 eV ($\sim$500 vibrational quanta) of vibrational energy into C_{60} in just two vibrational periods [Fig. 4(a)]. Physically, the first pulse forms a low amplitude wave packet and each successive pulse amplifies the wave packet, allowing efficient energy coupling into the system. In the second example we deal with the vibrational excitation induced by sudden ionization of $C_{60} \rightarrow C_{60}^{12+}$. Since the energy coupled to the molecule by rapid charging appears to limit the charge state that we can produce, a control pulse may allow us to form metastable C_{60}^{z+} with $z > 12$. A single control pulse timed to catch the wave packet on its return (at 3/4 the A_g period) will remove 50% of the vibrational energy from the molecule [Fig. 4(b)]. In this case the control pulse is circularly polarized to match the symmetric A_g wave packet better.

A general strategy for controlling coherent internal excitation in molecules is clear. Launch a large excursion vibrational wave packet by Frank-Condon overlap to an electronically excited state. If the dominant mode can be identified then a control pulse can be timed to work with it or against it. This approach to control works on the time scale less than a vibrational period and it can couple many eV's of energy into (or out of) the molecule, precisely and rapidly.

We are grateful for the expert technical assistance of D. Joines and J. P. Parsons.

[1] R. J. Levis, G. M. Menkir, and H. Rabitz, Science **292**, 709 (2001).
[2] A. Assion, T. Baumert, M. Bergt, T. Brixner, B. Kiefer, V. Seyfried, M. Strehle, and G. Gerber, Science **282**, 919 (1998).
[3] R. Judson and H. Rabitz, Phys. Rev. Lett. **68**, 1500 (1992).
[4] A. Zavriyev, P. H. Bucksbaum, H. G. Muller, and D. W. Schumaker, Phys. Rev. A **42**, 5500 (1990).
[5] R. Grimm, M. Weidemuller, and Y. B. Ovchinnikov, Adv. At. Mol. Opt. Phys. **42**, 95 (2000).
[6] S. Chu, J. E. Bjorkholm, A. Ashkin, and A. Cable, Phys. Rev. Lett. **57**, 314 (1986).
[7] H. Stapelfeldt, H. Sakai, E. Constant, and P. B. Corkum, Phys. Rev. Lett. **79**, 2787 (1997).
[8] D. M. Villeneuve, S. A. Aseyev, P. Dietrich, M. Spanner, M. Yu. Ivanov, and P. B. Corkum, Phys. Rev. Lett. **85**, 542 (2000).
[9] A. Ashkin, J. M. Dziedzic, and T. Yamane, Nature (London) **330**, 769 (1987).
[10] S. M. Block, Nature (London) **360**, 493 (1992).
[11] C. Guo, M. Li, J. P. Nibarger, and G. N. Gibson, Phys. Rev. A **58**, R4271 (1998).
[12] M. Lenzner, L. Kruger, S. Sartania, Z. Cheng, C. Spielmann, L. Mourou, W. Kautek, and F. Krausz, Phys. Rev. Lett. **80**, 4076 (1998).
[13] S. M. Hankin, D. M. Villeneuve, P. B. Corkum, and D. M. Rayner, Phys. Rev. Lett. **84**, 5082 (2000).
[14] M. Lezius, V. Blanchet, D. M. Rayner, D. M. Villeneuve, A. Stolow, and M. Y. Ivanov, Phys. Rev. Lett. **86**, 51 (2001).
[15] M. Tchaplyguine, K. Hoffmann, O. Dühr, H. Hohmann, G. Korn, H. Rottke, M. Wittmann, I. V. Hertel, and E. E. B. Campbell, J. Chem. Phys. **112**, 2781 (2000).
[16] E. E. B. Campbell, K. Hoffmann, H. Rottke, and I. V. Hertel, J. Chem. Phys. **114**, 1716 (2001).
[17] A. Brenac, F. Chandezon, H. Lebius, A. Pesnelle, S. Tomita, and B. Huber, Phys. Scr. **T80**, 195 (1999).
[18] S. M. Hankin, D. M. Villeneuve, P. B. Corkum, and D. M. Rayner, Phys. Rev. A **64**, 013405 (2001).
[19] S. Augst, D. Strikland, D. Meyerhofer, S. L. Chin, and J. Eberly, Phys. Rev. Lett. **63**, 2212 (1989).
[20] C. Yannouleas and U. Landman, Chem. Phys. Lett. **217**, 175 (1994).
[21] S. Matt, O. Echt, R. Wörgötter, V. Grill, C. Lifshitz, and T. D. Märk, Chem. Phys. Lett. **264**, 149 (1997).
[22] J. D. Jackson, *Classical Electrodynamics* (Wiley, New York, 1975), 2nd ed.
[23] D. E. Weeks and W. G. Harter, J. Chem. Phys. **90**, 4744 (1989).
[24] M. S. Dresselhaus, G. Dresselhaus, and P. C. Eklund, *Science of Fullerenes and Carbon Nanotubes* (Academic Press, San Diego, 1996).